Catalysis Science & Technology

Accepted Manuscript

ROYAL SOCIETY OF CHEMISTRY

www.rsc.org/catalysis

Xylan-type Hemicellulose Supported Palladium Nanoparticles: A Highly Efficient and Reusable Catalyst for the Carbon-Carbon Coupling Reactions

Wei Chen,[a] Lin-xin Zhong,[a] Xin-wen Peng,[*a] Kun-Wang,[b] Zhi-feng Chen,[a] and Run-cang Sun[*a,c]

a *State Key Laboratory of Pulp and Paper Engineering, South China University of Technology, Guangzhou 510641, China.*

b *School of Materials Science and Engineering, South China University of Technology, Guangzhou, 510641, China.*

c *Beijing Key Laboratory of Lignocellulosic Chemistry, Beijing Forestry University, Beijing 100083, China*.

* Corresponding authors. E-mail: fexwpeng@scut.edu.cn (Xin-wen Peng), or rcsun@scut.edu.cn (Run-cang Sun). Tel.: +86-010-62336972; Fax: +86-010-62336972.

Abstract

Palladium nanoparticles (PdNPs) were successfully prepared by using xylan-type hemicellulose (XH) as a support and used for the first time as an efficient and recyclable catalytic system in organic synthesis. The morphology, composition, and thermal stability of the catalyst were studied by means of TEM, XPS, XRD, FT-IR, and TGA. The as-prepared catalyst was further catalytically tested in various C−C cross-coupling reactions, and exhibited excellent catalytic activity in Suzuki, Heck, and Sonogashira coupling reactions. The catalyst could be easily recovered by simple filtration and reused for at least six times without significant loss of its catalytic activity. This work demonstrates the possibility of using XH as an efficient support for catalysis.

1. Introduction

The development of heterogeneous catalytic systems for fine chemicals synthesis has became a major research area. Conventionally, heterogeneous catalysis favors over homogeneous catalysis due to its many advantages, such as simple recovery and reusability.[1] However, the active sites in heterogeneous catalysts are typically less effective than those in homogeneous catalysts.[2] Integration of nanotechnology into ‘‘green chemistry’’ is one of the key issues in catalysis research today. Therefore, catalysis by metal nanoparticles (NPs) has attracted great interests from researchers.[3] This catalyst system, so-called “semi-heterogeneous catalysis”, is at the frontier between homogeneous catalysis and heterogeneous catalysis. This system not only shows high selectivity and efficiency but also possesses the ease of catalyst separation, recovery and recycling.[4]

Metal NPs have attracted great attention over the past decades owing to their unique electrical, optical, magnetic, and thermal properties.[5] In contrast to conventional catalysts, nanocatalysts exhibit high activity and selectivity, as well as excellent stability, due to their structural features such as small size and high surface-to-volume ratio.[6] These features make them particularly useful in various applications including biosensing, optical devices, medical dressings, and catalysis.[7] However, it is difficult to separate these tiny NPs from the reaction mixtures and reuse them again.[8] Thus, many attempts have been made to overcome above drawbacks by immobilizing the active species on supports with high surface area, such as silica,[9] carbon,[10] zeolite,[11] metal oxide,[12] polymers,[13] and nanocomposites.[14] Particularly,

sustainable and biodegradable natural polymers are attracting growing interest as substitutes for environmentally friendly catalyst supports. Among them, widely available polysaccharides represent attractive and promising biopolymers. Moreover, polysaccharides show many advantages that may stimulate their use as polymeric supports for catalysis: 1) they are the most abundant resources in the world, 2) they contain many reactive functional groups that can be used for anchoring NPs, and 3) they are chemically stable, biocompatible, and biodegradable.[15] However, natural polysaccharides used as capping agents for the stabilization of metal NPs for catalysis are still in their infancy. Recently, efforts have been devoted to using several biopolymers as environmentally benign catalyst supports, for instances, cellulose,[16] starch,[17] chitosan,[18] alginate,[19] guar-gum,[20] and β-cyclodextrin.[21]

Hemicelluloses (formed by different neutral sugar units such as xylose, arabinose, glucose, galactose, mannose, and also small quantity of D-glucuronic acid units), originating from trees, grasses, cereals, and other plants, are the second most common and abundant nature polymers.[22] So far, very little work has been carried out in which hemicelluloses were used as supports for the catalytic application. XH is the main hemicellulosic component of the cell walls of hardwoods and herbaceous plants (constituting about 20-35 wt% of the biomass).[23] In most cases, XH consists of a β (1→4)-D-xylopyranose backbone with side groups on the 2- or 3- position (Fig. 1). The electron-rich feature of hydroxyl and ether groups on XH chain make them suitable polymers for the preparation of metal NPs.[24] Furthermore, as a waste product from bio-refinery and pulp and paper industries, XH is available in large amounts but

has not been made the best of use yet.

Herein, we reported the use of XH as a promising support for PdNPs catalyst by a simple method: depositing PdNPs onto XH (PdNPs@XH). The applications of PdNPs@XH in Suzuki, Heck, and Sonogashira cross-coupling reactions under aerobic condition were investigated in detail.

2. Experimental Section

2.1 Materials

All chemicals were purchased from commercial suppliers (Aldrich, USA and Shanghai Chemical Company, China). XH was obtained from *Dendrocalamus membranaceus* Munro (*Dm*M) according to literature.[25] The sugar analysis showed the following sugar composition: 89.4% xylose, 5.8% arabinose, 1.9% glucose, 0.7% galactose, 1.8% glucuronic acid, 0.6% galactose acid.

2.2 Instruments

All ^{1}H spectra were recorded on Bruker FT-NMR (400 MHz) spectrometer and ^{13}C spectra were recorded on Bruker FT-NMR (100 MHz) spectrometer. NMR Chemical shifts were given as δ value (ppm) with reference to tetramethylsilane (TMS) as internal standard. The Pd content was determined by a Jarrell-Ash 1100 ICP analysis (ICP-AES). IR spectra were recorded on a Nicolet 6700 FT-IR spectrophotometer using KBr pellets. TEM images were captured with a JEOL-2010 transmission electron microscope. XRD measurements were carried out at room temperature using a Bruker D8 Advance X-ray powder diffractmeter. XPS measurements were performed on a Thermo Fisher Scientific (ESCALAB 250) instrument from VG

equipped with a hemispherical analyzer and an Al anode (monochromatic Kα X-rays at 1486.6 eV) used at 15 kV and 150W. TGA (TGA Q500, TA) was carried out in an aluminum crucible by heating to 700 ^{o}C at a heating rate of 20 ^{o}C min^{-1} with a nitrogen flow (25 mL min^{-1}). Products were purified by flash chromatography on 200-300 mesh silica gel, SiO_2.

2.3 Preparation of PdNPs@XH catalyst

PdNPs@XH catalyst was prepared by deposition-precipitation method as follows. Typically, 500 mg XH was dispersed in ethanol (100 mL), and 100 mg of $PdCl_2$ was quickly added under ultrasonication. Then to the reaction mixture, $NaBH_4$ (1.0 g) in deionized water (10 mL) was added over 0.5 h. After reaction for another 3 h, the solid product was filtered, and washed with water and ethanol for several times, and finally dried under vacuum at 80 ^{o}C to give dark catalyst PdNPs@XH with a Pd loading of 4.62 wt% calculated by inductively coupled plasma atomic emission spectroscopy (ICP-AES).

2.4 General Procedure for the Suzuki Coupling Reaction

Aryl halide (0.5 mmol), arylboronic acid (0.6 mmol), K_2CO_3 (1.0 mmol), and the supported palladium catalyst (PdNPs@XH, 11.5 mg containing 0.005 mmol Pd) were mixed in MeOH (2.0 mL), and then the mixture was heated at 50 ^{o}C under air atmosphere for 2 h. After that, the reaction solution was vacuum-filtered and washed with diethyl ether. Finally, the residue was concentrated and purified by flash chromatography on a silica gel using PE-EtOAc as an eluent to obtain the desired product. All the products were characterized by comparison of NMR spectral data

with the values of authentic samples. Spectral data of 4-Methoxybiphenyl (Table 1, entry 1, **3a**): ^{1}H NMR (400 MHz, $CDCl_3$): δ = 7.59–7.55 (m, 4H), 7.46–7.42 (m, 2H), 7.35–7.31 (m, 1H), 7.02–6.99 (m, 2H), 3.87 (s, 3H); ^{13}C NMR (100 MHz, $CDCl_3$): δ = 159.1, 140.8, 133.7, 128.7, 128.1, 126.7, 126.6, 114.2, 55.3.

2.5 General Procedure for the Heck Coupling Reaction

Aryl halide (0.5 mmol), vinyl substrate (0.6 mmol), NEt_3 (1.0 mmol), and the supported palladium catalyst (PdNPs@XH, 23 mg containing Pd 0.01 mmol) were mixed in CH_3CN (2.0 mL), and then the mixture was heated to reflux under air atmosphere for 8 h. After that, the reaction solution was vacuum-filtered and washed with diethyl ether. Finally, the residue was concentrated and purified by flash chromatography on a silica gel using PE-EtOAc as an eluent to obtain the desired product. All the products were characterized by comparison of NMR spectral data with the values of authentic samples. Spectral data of (*E*)-*n*-Butyl 3-(4-methoxyphenyl)-2-propenoate (Table 2, entry 3, **5c**): ^{1}H NMR (400 MHz, $CDCl_3$): δ = 7.64 (d, J = 16.0 Hz, 1H), 7.47 (d, J = 8.0 Hz, 2H), 6.89 (d, J = 8.0 Hz, 2H), 6.31 (d, J = 16.0 Hz, 1H), 4.19 (t, J = 8.0 Hz, 2H), 3.82 (s, 3H), 1.72–1.65 (m, 2H), 1.48–1.39 (m, 2H), 0.96 (t, J = 8.0 Hz, 3H); ^{13}C NMR (100 MHz, $CDCl_3$): δ = 167.3, 161.2, 144.1, 129.6, 127.1, 115.6, 114.2, 64.2, 55.2, 30.7, 19.1, 13.7.

2.6 General Procedure for the Sonogashira Coupling Reaction

Aryl halide (0.5 mmol), terminal alkyne (0.6 mmol), NEt_3 (1.0 mmol), and the supported palladium catalyst (PdNPs@XH, 23 mg containing Pd 0.01 mmol) were mixed in CH_3CN (2.0 mL), and then the mixture was heated to reflux under air

atmosphere for 6 h. After that, the reaction solution was vacuum-filtered and washed with diethyl ether. Finally, the residue was concentrated and purified by flash chromatography on a silica gel using PE-EtOAc as an eluent to obtain the desired product. All the products were characterized by comparison of NMR spectral data with the values of authentic samples. Spectral data of 1-(4-Methoxyphenyl)-1-hexyne (Table 3, entry 6, **7e**): ^{1}H NMR (400 MHz, $CDCl_3$): δ = 7.33−7.31 (m, 2H), 6.81−6.79 (m, 2H), 3.78 (s, 3H,), 2.38 (t, J = 8.0 Hz, 2H), 1.61−1.54 (m, 2H), 1.51−1.44 (m, 2H), 0.94 (t, J = 8.0Hz, 3H); ^{13}C NMR (100 MHz, $CDCl_3$): δ = 158.9, 132.8, 116.2, 113.7, 88.7, 80.2, 55.2, 30.9, 22.0, 19.1, 13.6.

3. Results and Discussion

3.1 Characterization of the PdNPS@XH

The whole preparation route of PdNPs@XH including two steps was illustrated in Scheme 1. First, XH was mixed with a $PdCl_2$ aqueous solution at room temperature. The mixture instantly turned from pale yellow to pale brown, indicating the coordination of metal salts to XH.[26] Second, followed by $NaBH_4$ reduction, the solution turned dark gray, indicating the reduction of Pd(II) salts into Pd(0) NPs, generating Pd(0) NPs decorated XH composites.

Fig. 2 showed the morphology of the hybrid NPs. It was easily observed in Fig. 2a that a large number of PdNPs were formed and uniformly distributed on the surface of XH after deposition. The as-prepared Pd NPs had a broad size distribution with diameter ranging from 8 to 18 nm according to the particle size distribution histogram, and the average particle size was about 12 nm. As illustrated in Fig. 2b, some small

PdNPs (about 12 nm) dispersed on the surface of XH were found to aggregate into clusters with different dimensions, and the size of PdNPs did not increase after reaction. XRD patterns of catalysts before and after reaction showed that the characteristic peaks of Pd(0) did not change, except the weak intensity of the reused catalyst (Fig. 3b and 3c). The energy dispersive analysis of X-rays for the selected areas further revealed the elemental composition of the supported catalyst. As shown in Fig. 2c, the element Pd presented in both fresh and reused catalyst, clearly confirming that the darker spots on the XH were PdNPs. The lattice fringes of Pd were also detected and shown in Fig. 2d. The interplanar distance was about 0.22 nm, which corresponds well with the (111) lattice plane of Pd.[27]

The crystallinity and phase composition of the resulting products were determined by XRD. From the XRD spectra shown in Fig. 3a, there was a broad diffraction peak at 2θ = 10-20°, which is typically attributed to amorphous XH.[28] On the XRD patterns of PdNPs@XH shown in Fig. 3b, the peaks observed at 2θ = 40.1°, 46.6°, and 68.2°, which are characteristic peaks of Pd(0) and can be assigned to the (111), (200), and (220) planes of Pd crystal.[29] All of the diffraction peaks match well with those of the face-centered cubic (fcc) Pd crystal structure. It was worth to note that the broad diffraction peak at 2θ = 10-20° still existed in the XRD spectra of PdNPs@XH and recycled PdNPs@XH, indicating the deposition of PdNPs on XH and reuse of catalyst did not change the crystallographic behavior of XH scaffold.

Fig. 4 exhibited the FT-IR spectra of XH and PdNPs@XH. In the spectrum of XH (Fig. 4a), the broad peaks at around 3445 and 2926 cm^{-1} are assigned to O-H and C-H

stretching vibrations, the prominent absorption at 1045 cm^{-1} originates from C-O-C in glycosidic linkage, and the sharp band at 889 cm^{-1} is due to *β*-glycosidic linkage between sugar units, well agreeing with the results reported in literature.[30] The relatively strong absorption at around 1641 cm^{-1} indicates the characteristic peak of C=O mainly from 4-*O*-methyl-glucuronic acid branches.[31] PdNPs@XH catalyst exhibited similar FT-IR spectra to XH scaffold in terms of characteristic peaks, which indicated that the deposition of PdNPs on XH surface via physical bonding did not change the original structure of XH, in agreement with the results observed from XRD.

XPS analysis was also performed to confirm the complete reduction of Pd(II). Fig. 5 showed the high-resolution XPS Pd 3d spectrum in PdNPs@XH. The binding energy of the doublet peaks at 335.4 eV (assigned to Pd 3d5/2) and 340.3 eV (assigned to Pd 3d3/2) can be attributed to Pd(0) state.[32] This results indicated that the Pd species on XH was Pd(0) state and no Pd(II) state existed in the PdNPs@XH composites. The inset image showed the survey spectrum of PdNPs@XH composites. The signal of Pd was weaker than those of elements O and C, because XH was not fully covered by PdNPs.

Generally, heating conditions are necessary in Suzuki, Heck and Sonogashira cross-coupling reactions. Hence, the thermal property of catalyst has a great impact on its catalytic activity and recyclability. The thermal stability of the XH scaffold and PdNPs@XH were studied by thermal gravimetric analysis (TGA) in nitrogen flow. As indicated in Fig. 6, PdNPs@XH exhibited the same thermal stability as XH scaffold,

evidenced that the deposition of PdNPs on XH did not alter the thermal behavior of XH, both XH and PdNPs@XH decomposed above 220 ^{o}C under inert atmosphere. It was noted that PdNPs@XH exhibited about 5% higher residual weight than XH.

3.2 Catalytic activity

To evaluate the putative catalytic activity of PdNPs@XH, Suzuki, Heck, and Sonogashira cross-coupling reactions were carried out as model reactions. These reactions are generally catalyzed by soluble Pd complexes with various ligands. However, the efficient separation and subsequent recycle of catalyst remain scientific challenges. In this study, we demonstrated PdNPs@XH as a heterogeneous catalyst for these reactions.

In order to optimize the reaction conditions, 4-iodoanisole was selected as a substrate, and the reactions were summarized in Scheme 2. After screening a range of usual inorganic and organic bases and exploring the scopes of various solvents, we found that PdNPs@XH was the most effective for Suzuki reaction when using K_2CO_3 as base and MeOH as solvent at 50 ^{o}C. Heck and Sonogashira reactions proceeded well in the presence of NEt_3 as base and CH_3CN as solvent. To examine the scopes of Suzuki, Heck, and Sonogashira coupling reactions, we extended our study to different combinations of aryl halides with aryl boronic acids, alkenes, and alkynes under the optimized reaction condition, respectively. The results were listed in Tables 1–3.

Indeed, PdNPs@XH was proved to be an effective catalyst for Suzuki coupling reaction as shown in Table 1. A diverse array of aryl iodides and aryl bromides in the reaction with phenylboronic acid exhibited high reactivity and good to excellent

yields of biphenyls products were obtained as indicated by Table 1 (entries1–4). However, the coupling reaction of aryl chlorides, such as 4-nitrochlorobenzene and 4-chloroanisole, with phenylboronic acid gave poor results (Table 1, entries 5 and 6). By the way, arylboronic acids bearing electron-withdrawing and -donating groups, also coupled efficiently with 4-bromoanisole, and the excellent yields of the corresponding products were isolated (Table 1, entries 7 and 8).

Heck coupling reactions of various aryl iodides and aryl bromides with vinyl substrates were also performed by using PdNPs@XH as catalyst (Table 2). The coupling reactions proceeded smoothly and generated the corresponding products in good to excellent yields (Table 2, entries 1–4). As for aryl chlorides, both electron-withdrawing and -donating groups in substrates were investigated. Unfortunately, no Heck products were detected even changing solvent, increasing reaction temperature and reaction time (Table 2, entries 5 and 6). Meanwhile, the scope of this catalytic system with vinyl substrates including methyl acrylate, ethyl acrylate, and styrene was also examined. Methyl acrylate, ethyl acrylate gave higher yields than styrene (Table 2, entries 7 and 8), which may be related to their molecule structures.

Encouraged by the above results from Suzuki and Heck reactions, PdNPs@XH was also explored for Sonogashira reaction using a variety of substrates. As illustrated in Table 3, the results were similar to Heck reactions, aryl iodides and aryl bromides efficiently reacted with phenylacetylene to yield Sonogashira products (Table 3, entries 1–4). For aryl chloride, however, the catalytic system did not work for

Sonogashira reaction (Table 3, entries 5 and 6). On the other hand, as for the scope of terminal alkyne, both aromatic alkynes and aliphatic alkynes could be coupled smoothly with 4-iodoanisole and produce the desired products in good yields (Table 3, entries 7 and 8).

Isolation and reuse of catalyst are crucial requirements for practical applications. In this work, the reaction solution was vacuum filtered and the supported catalyst was filtered off and washed with EtOH, H_2O, and Et_2O, respectively. Then the filter cake was dried in air and reused directly without further purification. In order to test the reusability of PdNPs@XH, the model reactions of Suzuki, Heck, and Sonogashira coupling reactions were chosen. As summarized in Table 4, the catalyst could be recycled and reused for at least six consecutive trials with no obvious decrease in conversion and selectivity. Furthermore, metal leaching was another concern for the heterogeneous catalyst. In this study, the Pd leaching from the support after six cycles was analyzed by ICP-AES and the results were listed in Table 4. In Suzuki reaction, the Pd loss amount was only 0.18%, while 0.46% was detected in Heck and Sonogashira reactions. Based on the results from TEM and XRD, the agglomeration and leaching of Pd should be responsible for the decreasing catalytic activity of the recovered catalyst and the slightly decreasing yield with recycle.

We compared the results achieved in this work with other biopolymers-based catalysts and common carbon materials supported catalysts for Suzuki, Heck, and Sonogashira coupling reactions, and the results were listed in Table 5. In comparison with other catalysts employed for the synthesis 4-methoxybiphenyl from

4-bromoanisole and phenylbronic acid, PdNPs@XH showed a much higher catalytic activity in terms of mild reaction conditions and high yield (Table 5, entries 1–4). As for Heck reaction, taking iodobenzene reacting with styrene as an example, the results were listed in Table 5, entries 5–10. It could be seen that the catalysts obtained in this study were superior to others except for entries 6 and 7 in Table 5. Although high yields were obtained by employing high-boiling solvent DMF, but product purification is still a challenge. To compare the efficiency of our catalyst with those of other catalysts reported for Sonogashira reaction, we chose the reaction between iodobenzene and phenylacetylene. As it is shown in Table 5, entries 11–14, our catalyst showed some extent improvement in reaction conditions, such as reaction temperature, reaction time and yield. For example, catalysts prepared from CELL-Pd(0) afforded the much longer reaction time, although the high yield obtained from Sonogashira reaction (entry 11 in Table 5). Catalysis for Suzuki, Heck, and Sonogashira reactions by utilizing renewable XH from biomass presents an ideal chemical process. This type of reaction is very important in terms of "Green Chemistry" since waste can be decreased in the absence of ligand and at low palladium loading. These advantages can be extended to other types of catalysis.

4. Conclusions

In summary, we have developed a highly effective Pd(0) nanocatalyst immobilized on xylan-type hemicellulose for Suzuki, Heck, and Sonogashira carbon-carbon cross-coupling reactions. A wide range of substrates were coupled successfully under aerobic conditions. More importantly, the catalyst exhibited high catalytic activity and

stability, and could be reused for at least six times without significant loss of its catalytic activity. XH thus was proved to be a promising support for catalysis, with good thermal and chemical stability.

Acknowledgements

The authors are extremely grateful to financial support from the State Key Program of National Natural Science Foundation of China (No. 21336002), Guangdong natural Science Foundation (S2013040015055), Fundamental Research Funds for the Central Universities (2013ZM0050), Science and Technology Project of Guangzhou City in China, National Natural Science Foundation of China (31110103902), Major State Basic Research Projects of China (973-2010CB732204).

References

1 a) M. J. Jin and D. H. Lee, *Angew. Chem., Int. Ed*., 2010, **49**, 1119–1122; b) L. Yin and J. Liebscher, *Chem. Rev*., 2007, **107**, 133–173.

2 a) R. Abu-Reziq, H. Alper, D. Wang and M. L. Post, *J. Am. Chem. Soc*., 2006, **128**, 5279–5282; b) A. S. K. Hashmi and G. J. Hutchings, *Angew. Chem., Int. Ed*., 2006, **45**, 7896–7936.

3 J. Grunes, J. Zhu and G. A. Somorjai, *Chem. Commun*., 2003, 2257–2260.

4 D. Astruc, F. Lu and J. R. Aranzaes, *Angew. Chem., Int. Ed*., 2005, **44**, 7852–7872.

5 a) X. Michalet, F. F. Pinaud, L. A. Bentolila, J. M. Tsay, S. Doose, J. J. Li, G. Sundaresan, A. M. Wu, S. S. Gambhir and S. Weiss, *Science*, 2005, **307**, 538–544; b) A. Nel, T. Xia, L. Madler and N. Li, *Science*, 2006, **311**, 622–627.

6 G. A. Somorjai, H. Frei and J. Y. Park, *J. Am. Chem. Soc.*, 2009, **131**, 16589–16605.

7 a) C. A. Mirkin, R. L. Letsinger, R. C. Mucic and J. J. Storhoff, *Nature*, 1996, **382**, 607–609; b) S. Perni, P. Prokopovich, J. Pratten, I. P. Parkin and M. Wilson, *Photochem. Photobiol. Sci.*, 2011, **10**, 712–720; c) S. Shiv Shankar, A. Rai, A. Ahmad and M. Sastry, *Chem. Mater.*, 2005, **17**, 566–572; d) D. T. Nguyen, D. J. Kim and K. S. Kim, *Micron.*, 2011, **42**, 207–227.

8 M. Beller, H. Fischer, K. Kuhlein, C. P. Reisinger and W. A. Herrmann, *J. Organomet. Chem.*, 1996, **520**, 257–259.

9 a) R. B. Bedford, U. G. Singh, R. I. Walton, R. T. Williams and S. A. Davis, *Chem. Mater.*, 2005, **17**, 701–707; b) X. Liu, A. Wang, X. Yang, T. Zhang, C. Y. Mou, D. S. Su and J. Li, *Chem. Mater.*, 2009, **21**, 410–418.

10 a) S. H. Joo, S. J. Choi, I. Oh, J. Kwak, Z. Liu, O. Terasak and R. Ryoo, *Nature*, 2001, **412**, 169–172; b) N. N. Kariuki, X. Wang, J. R. Mawdsley, M. S. Ferrandon, S. G. Niyogi, J. T. Vaughey and D. J. Myers, *Chem. Mater.*, 2010, **22**, 4144–4152.

11 a) L. Gu, D. Ma, S. Yao, C. Wang, W. Chen and X. Bao, *Chem. Commun.*, 2010, **46**, 1733–1735; b) M. Iwasaki and H. Shinjoh, *Chem. Commun.*, 2011, **47**, 3966–3968.

12 K. Zorn, S. Giorgio, E. Halwax, C. R. Henry, H. Grönbeck and G. Rupprechter, *J. Phys. Chem. C*, 2011, **115**, 1103–1111.

13 a) R. N. Dhital, C. Kamonsatikul, E. Somsook, K. Bobuatong, M. Ehara, S. Karanjit and H. Sakurai, *J. Am. Chem. Soc.*, 2012, **134**, 20250–20253; b) J. Zhang, D. Han, H. Zhang, M. Chaker, Y. Zhao and D. Ma, *Chem. Commun.*, 2012, **48**, 11510–11512.

14 A. K. Diallo, C. Ornelas, L. Salmon, J. R. Aranzaes and D. Astruc, *Angew. Chem., Int. Ed.*, 2007, **46**, 8644–8648.

15 T. Heinze, in *Polysaccharides: Structural Diversity and Functional Versatility*, ed. S. Dumitriu, Marcel Dekker, New York, 2005.

16 a) C. M. Cirtiu, A. F. Dunlop-Brière and A. Moores, *Green Chem.*, 2011, **13**, 288–291; b) H. Koga, A. Azetsu, E. Tokunaga, T. Saito, A. Isogai and T. Kitaoka, *J. Mater. Chem.*, 2012, **22**, 5538–5542.

17 M. J. Gronnow, R. Luque, D. J. Macquarrie and J. H. Clark, *Green Chem.*, 2005, **7**, 552–557.

18 a) M. Chtchigrovsky, A. Primo, P. Gonzalez, K. Molvinger, M. Robitzer, F. Quignard and F. Taran, *Angew. Chem., Int. Ed.*, 2009, **48**, 5916–5920; b) R. B. N. Baig and R. S. Varma, *Green Chem.*, 2013, **15**, 1839–1843.

19 A. Primo, M. Liebel and F. Quignard, *Chem. Mater.*, 2009, **21**, 612–627.

20 A. Kumar, S. Aerry, A. Saxena, A. de and S. Mozumdar, *Green Chem.*, 2012, **14**, 1298–1301.

21 a) B. Kaboudin, R. Mostafalu and T. Yokomatsu, *Green Chem.*, 2013, **15**, 2266–2274; b) N. T. T. Chau, S. Handjani, J.-P. Guegan, M. Guerrero, E. Monflier, K. Philippot, A. Denicourt-Nowicki and A. Roucoux, *ChemCatChem*, 2013, **5**, 1497–1503.

22 R. C. Sun, X. F. Sun and J. Tomkinson in *Hemicellulose: Science and Technology*, ed. P. Gatenholm and M. Tenkanen, American Chemical Society, Washington, DC, 2004.

23 T. Heinze, A. Koschella and A. Ebringerová in *Hemicelluloses: Science and Technology*, ed. P. Gatenholm and M. Tenkanen, ACS Symposium Series 864, American Chemical Society, Washington, 2004.

24 Y. Habibi and A. Dufresne, *Biomacromolecules*, 2008, **9**, 1974–1980.

25 X. W. Peng, J. L. Ren, L. X. Zhong and R. C. Sun, *J. Agric. Food Chem.*, 2012, **60**, 1695–1702.

26 P. Klufers and T. Kunte, *Chem. Eur. J.*, 2003, **9**, 2013–2018.

27 R. Li, P. Zhang, Y. M. Huang, P. Zhang, H. Zhong and Q. W. Chen, *J. Mater. Chem.*, 2012, **22**, 22750–22755.

28 X. W. Peng, J. L. Ren, L. X. Zhong and R. C. Sun, *Biomacromolecules*, 2011, **12**, 3321–3329.

29 S. U. Son, Y. Jang, J. Park, H. B. Na, H. M. Park, H. J. Yun, J. Lee and T. Hyeon, *J. Am. Chem. Soc.*, 2004, **126**, 5026–5027.

30 N. Blumenkrantz and G. Asboe-Hanson, *Anal. Biochem.*, 1973, **54**, 484–489.

31 A. K. Chatjigakis, C. Pappas, N. Proxenia, O. Kalantzi, P. Rodis and M. Polissiou, *Carbohydr. Polym.*, 1998, **37**, 395–408.

32 C. Evangelisti, N. Panziera, P. Pertici, G. Vitulli, P. Salvadori, C. Battocchio and G. Polzonetti, *J. Catal.*, 2009, **262**, 287–293.

33 a) N. Jamwal, R. K. Sodhi, P. Gupta and S. Paul, *Int. J. Biol. Macromol.*, 2011, **49**, 930–935; b) Q. Du and Y. Li, *Beilstein J. Org. Chem.*, 2011, **7**, 378–385; c) P. P. Zhou, H. H. Wang, J. Z. Yang, J. Tang, D. P. Sun and W. H. Tang, *Ind. Eng. Chem. Res.*, 2012, **51**, 5743−5748; d) K. R. Reddy, N. S. Kumar, P. S. Reddy, B. Sreedhar and M.

L. Kantam, *J. Mol. Catal. A: Chem.*, 2006, **252**, 12−16; e) W. J. Sun, Z. Q. Liu, C. F. Jiang, Y. Xue, W. Chu and X. S. Zhao, *Catal. Today*, 2013, **212**, 206−214; f) L. P. Chen, S. G. Hong, X. P. Zhou, Z. P. Zhou and H. Q. Hou, *Catal. Commun.*, 2008, **9**, 2221–2225.

419 **Table 1** Suzuki coupling reactions of aryl halide with arylboronic acid.[a]

420 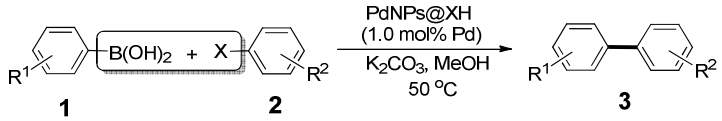

Entry	Arylboronic acid	Aryl halide	Product **3**	Yield[b] (%)
1	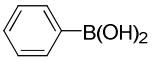	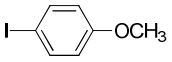	**3a**	99
2	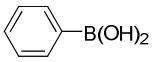	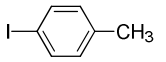	**3b**	98
3	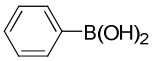	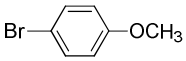	**3c**	96
4	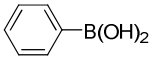	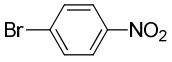	**3d**	97
5[c]	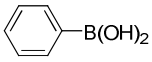	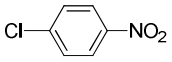	**3d**	5
6[c]	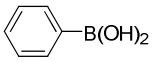	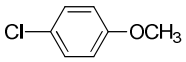	**3c**	trace
7	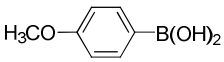	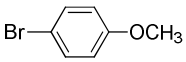	**3e**	94
8	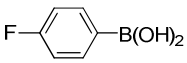	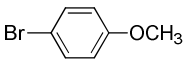	**3f**	88

421 [a] Reaction conditions: 0.5 mmol aryl halide, 0.6 mmol arylboronic acid, 11.5 mg
422 PdNPs@XH (containing 0.005 mmol Pd), 1.0 mmol K_2CO_3, 2.0 mL MeOH, 50 °C, 2
423 h.

424 [b] Isolated yields.

425 [c] Reaction conditions: 0.5 mmol aryl chloride, 0.6 mmol arylboronic acid, 11.5 mg
426 PdNPs@XH (containing 0.005 mmol Pd), 1.0 mmol K_2CO_3, 2.0 mL DMF, 70 °C, 5 h.
427 Products determined by GC.

428

Table 2 Heck coupling reactions of aryl halide with alkene.[a]

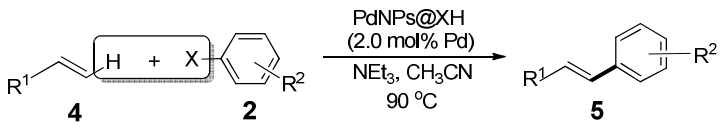

Entry	Alkene	Aryl halide	Product **5**	Yield[b] (%)
1	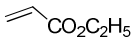	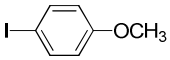	**5a**	99
2	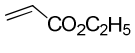	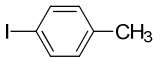	**5b**	98
3	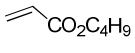	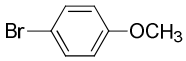	**5c**	94
4	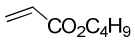	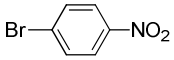	**5d**	96
5[c]	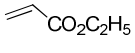	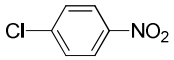	**5e**	NR
6[c]	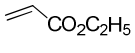	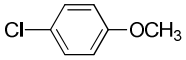	**5a**	NR
7	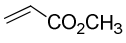	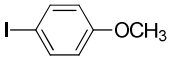	**5f**	95
8		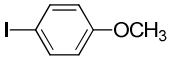	**5g**	86

[a] Reaction conditions: 0.5 mmol aryl halide, 0.6 mmol vinyl substrate, 23 mg PdNPs@XH (containing Pd 0.01 mmol), 1.0 mmol NEt_3 , 2.0 mL CH_3CN, 90 °C, 8 h.

[b] Isolated yields.

[c] Reaction conditions: 0.5 mmol aryl chloride, 0.6 mmol vinyl substrate, 23 mg PdNPs@XH (containing 0.01 mmol Pd), 1.0 mmol NEt_3 , 2.0 mL DMF, 120 °C, 10 h.

439 **Table 3** Sonogashira coupling reactions of aryl halide with terminal alkyne.[a]

440 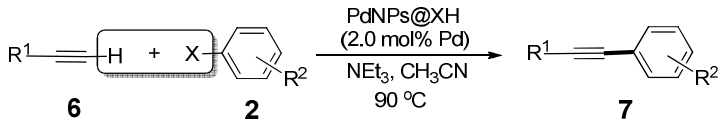

6 2 7

Entry	Alkyne	Aryl halide	Product **7**	Yield[b] (%)
1	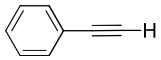	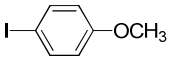	**7a**	96
2	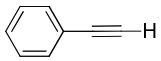	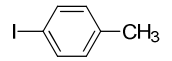	**7b**	95
3	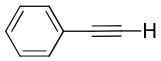	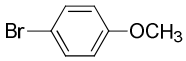	**7a**	92
4	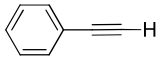	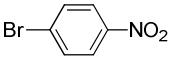	**7c**	94
5[c]	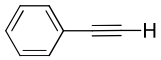	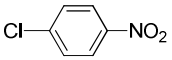	**7c**	NR
6[c]	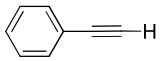	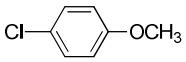	**7a**	NR
7	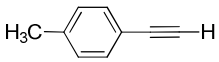	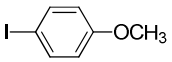	**7d**	94
8		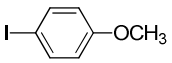	**7e**	82

441 [a] Reaction conditions: 0.5 mmol aryl halide, 0.6 mmol terminal alkyne, 23 mg
442 PdNPs@XH (containing 0.01 mmol Pd), 1.0 mmol NEt_3, 2.0 mL CH_3CN, 90 °C, 6 h.
443 [b] Isolated yields.
444 [c] Reaction conditions: 0.5 mmol aryl chloride, 0.6 mmol terminal alkyne, 23 mg
445 PdNPs@XH (containing 0.01 mmol Pd), 1.0 mmol NEt_3, 2.0 mL DMF, 120 °C, 10 h.
446
447
448

Table 4 Catalytic performances of PdNPs@XH and Pd leaching in successive Suzuki, Heck, and Sonogashira reactions runs.[a]

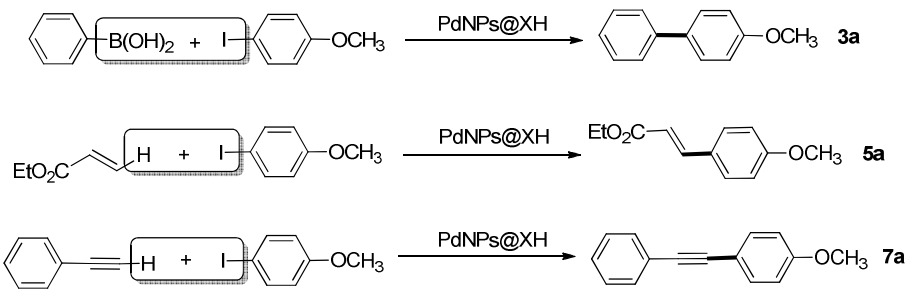

Trial	Yield[b] (%) of **3a**	Yield[b] (%) of **5a**	Yield[b] (%) of **7a**
1	99	99	96
2	99	96	94
3	97	94	92
4	94	95	88
5	95	93	90
6	93	90	87
Pd leaching after 6 cycles[c]	0.18	0.46	0.46

[a] Suzuki coupling reaction conditions: 0.5 mmol 4-iodoanisole, 0.6 mmol phenylboronic acid, 11.5 mg PdNPs@XH (containing 0.005 mmol Pd), 1.0 mmol K_2CO_3 , 2.0 mL MeOH, 50 ^oC, 2 h; Heck coupling reaction conditions: 0.5 mmol 4-iodoanisole, 0.6 mmol ethyl acrylate, 23 mg PdNPs@XH (containing 0.01 mmol Pd), 1.0 mmol NEt_3, 2.0 mL CH_3CN, 90 ^oC, 8 h; Sonogashira coupling reaction conditions: 0.5 mmol 4-iodoanisole, 0.6 mmol phenylacetylene, 23 mg PdNPs@XH (containing 0.01 mmol Pd), 1.0 mmol NEt_3, 2.0 mL CH_3CN, 90 ^oC, 6 h.

460 [b] Isolated yields.

461 [c] Pd content in product phase in % of the initial Pd loading of the catalysts.

462

463

464

465

466

467

468

469

470

471

472

473

474

475

476

477

478

479

480

481

Table 5 Catalytic performances of different Pd-based catalysts in Suzuki, Heck, and Sonogashira coupling reaction.

Entry	Coupling Reactions	Catalyst	Solvent	*T* (°C)	*t* (h)	Yield (%)	Ref.
1	Suzuki	CELL-Pd(0) [a]	H_2O	100	7	83	33a
2	Suzuki	Cell-$OPPh_2$-Pd^0 [b]	95% C_2H_5OH	reflux	0.4	75	33b
3	Suzuki	Pd/C [c]	CH_3OH	50	2	78	This work
4	Suzuki	PdNPs@XH	CH_3OH	50	2	96	This work
5	Heck	PdNPs@CNCs [d]	CH_3CN/H_2O1:1	100	24	75	16a
6	Heck	Pd/BC [e]	DMF	120	8	97	33c
7	Heck	CELL-Pd(0) [a]	DMF	120	12	100	33d
8	Heck	Pd/CNTs [f]	DMF	100	5	82	33e
9	Heck	Pd/C [c]	CH_3CN	90	8	85	This work
10	Heck	PdNPs@XH	CH_3CN	90	8	92	This work
11	Sonogashira	CELL-Pd(0) [a]	CH_3CN	reflux	12	96	33d
12	Sonogashira	Pd-NP/CEPFs [f]	H_2O	reflux	3	88	33f
13	Sonogashira	Pd/C [c]	CH_3CN	90	6	78	This work
14	Sonogashira	PdNPs@XH	CH_3CN	90	6	96	This work

[a]. Pd nanoparticles supported on cellulose.

[b]. Pd nanoparticles supported on phosphine functionalized cellulose.

[c]. Commercial sources.

[d]. Pd nanoparticles supported on cellulose nanocrystallites.

[e]. Pd nanoparticles supported on bacteria cellulose.

489 [f]. Pd nanoparticles supported on carbon nanotubes.

490

491

492

493

494

495

496

497

498

499

500

501

502

503

504

505

506

507

508

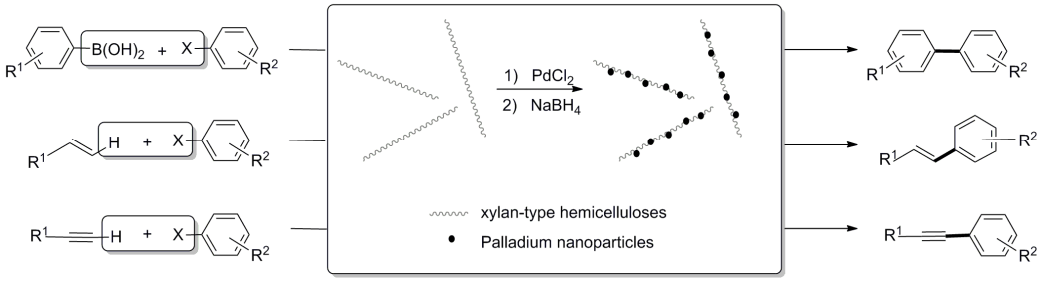

Scheme 1 Preparation of the xylan-type hemicellulose supported palladium catalyst and its applications in Suzuki, Heck, and Sonogashira reactions.

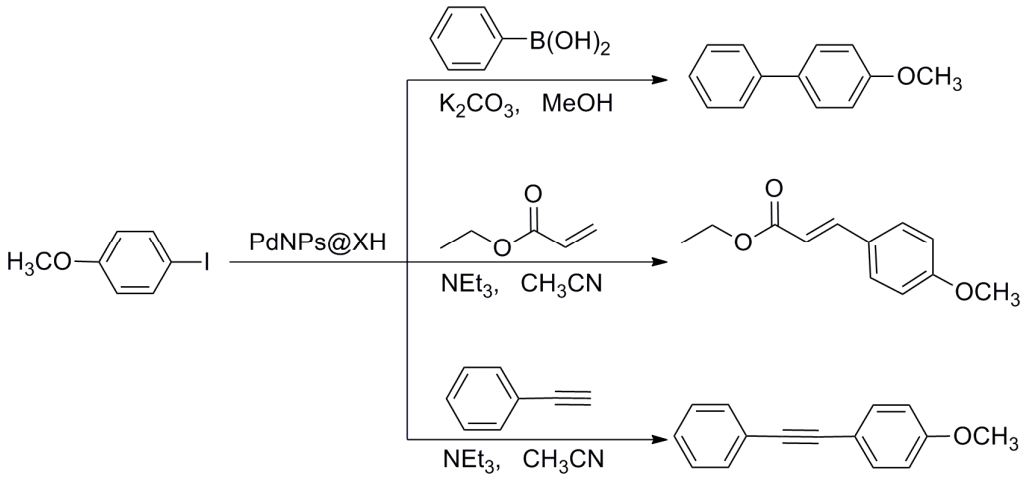

Scheme 2 PdNPs@XH catalyzed Suzuki, Heck, and Sonogashira reactions.

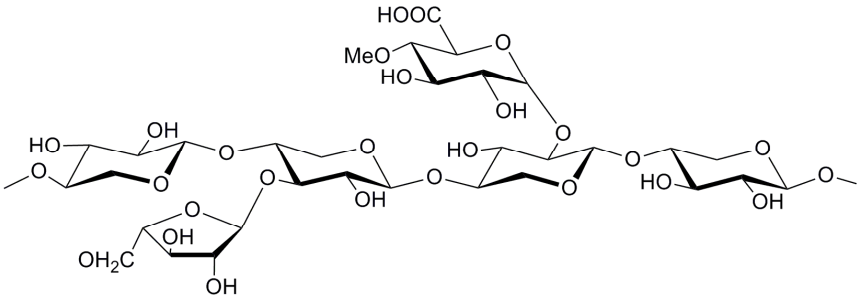

Fig. 1 Represent structure of xylan-type hemicellulose

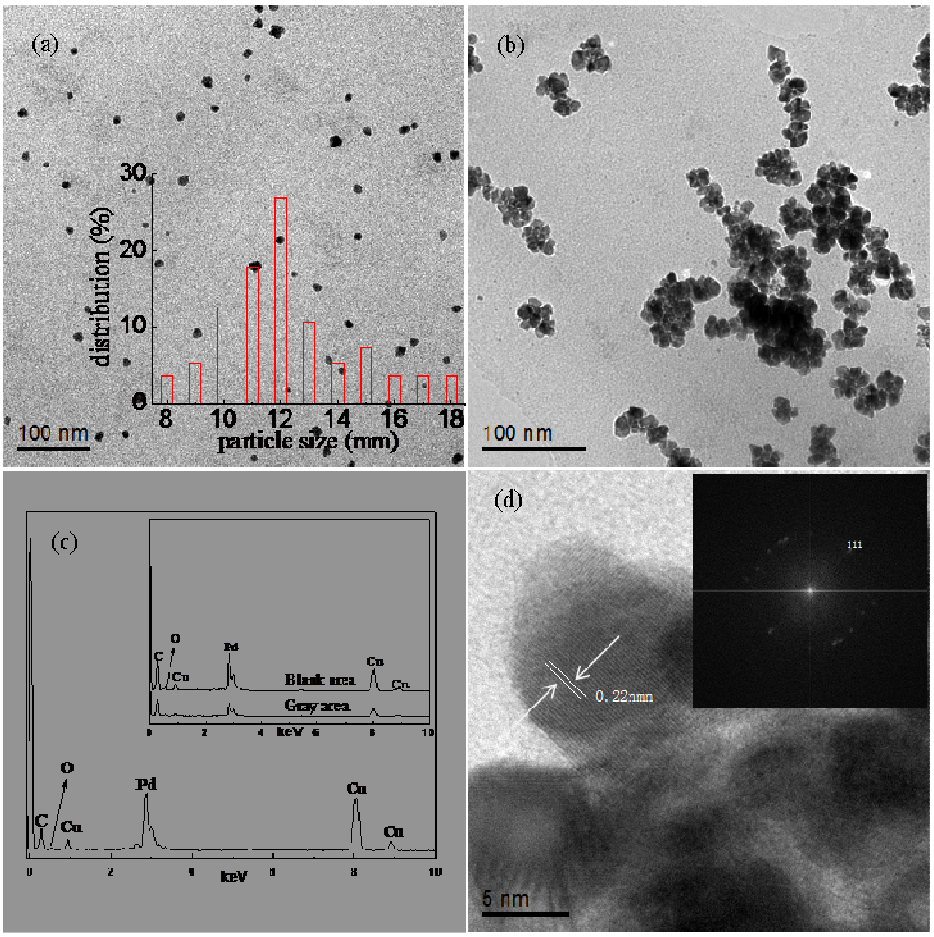

Fig. 2 TEM images: (a) Fresh PdNPs@XH and particle size distribution histogram; (b) The reused PdNPs@XH originated from Suzuki reaction for six times; (c) EDAX of PdNPs@XH and reused PdNPs@XH originated from Suzuki reaction; (d) Lattice fringe of Pd nanoparticles

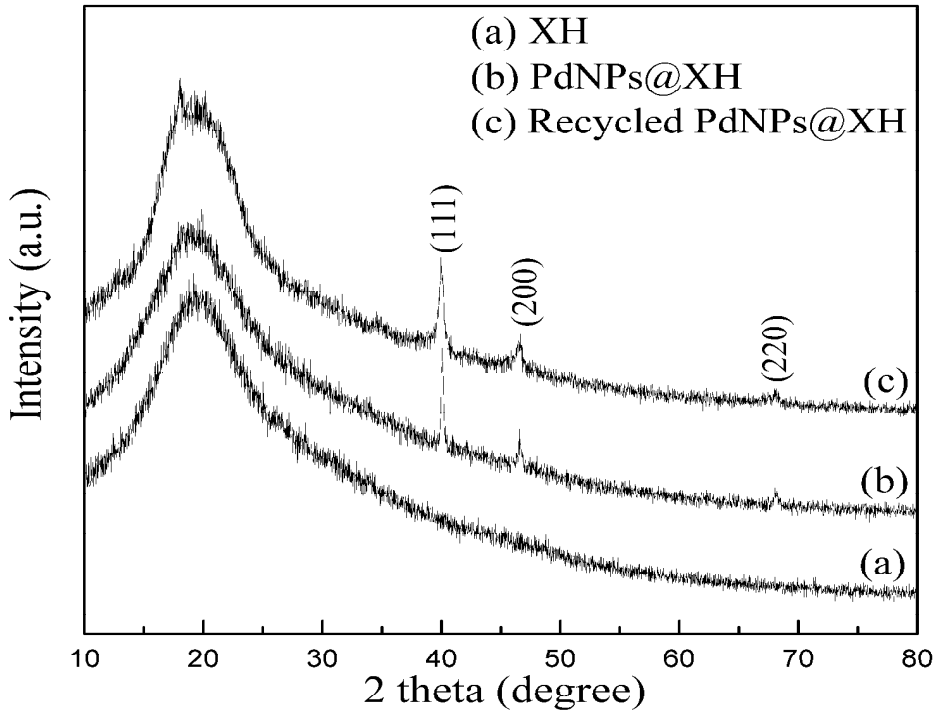

598

599 **Fig. 3** XRD of XH, PdNPs@XH and recycled PdNPs@XH

600
601
602
603
604
605
606

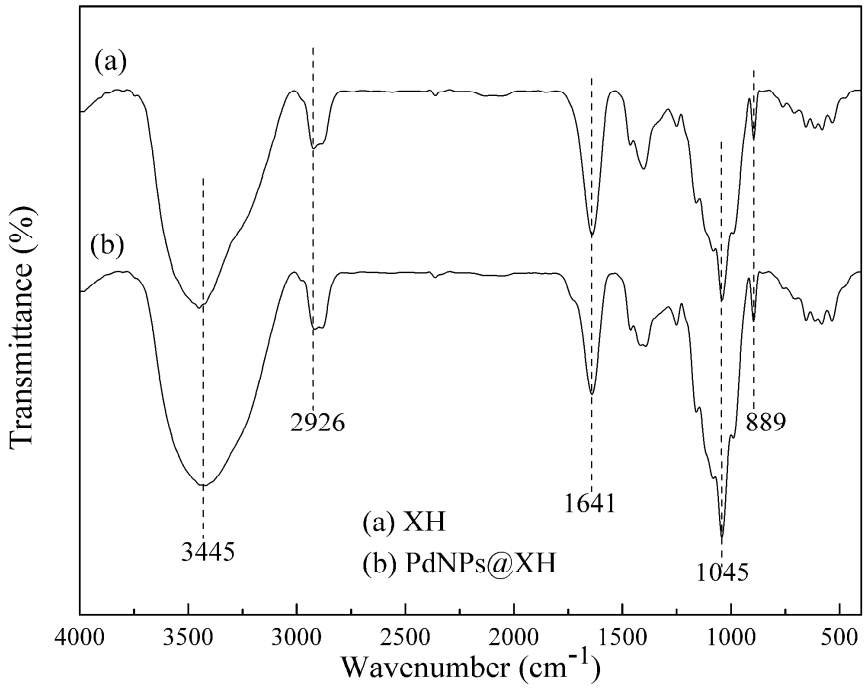

607

608 **Fig. 4** FT-IR spectra of XH and PdNPs@XH

609

610

611

612

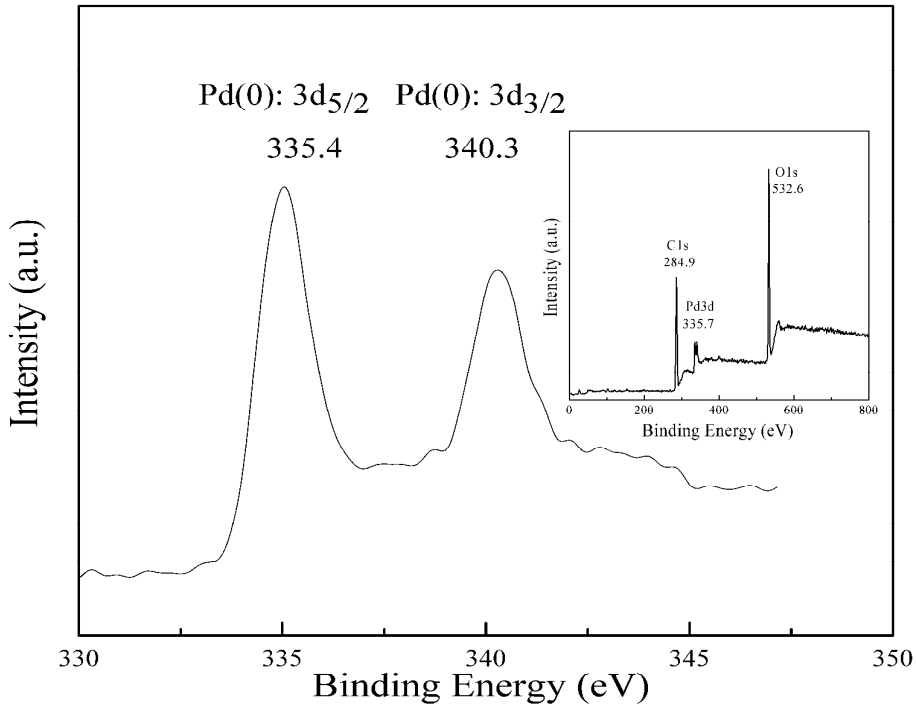

Fig. 5 XPS of PdNPs@XH

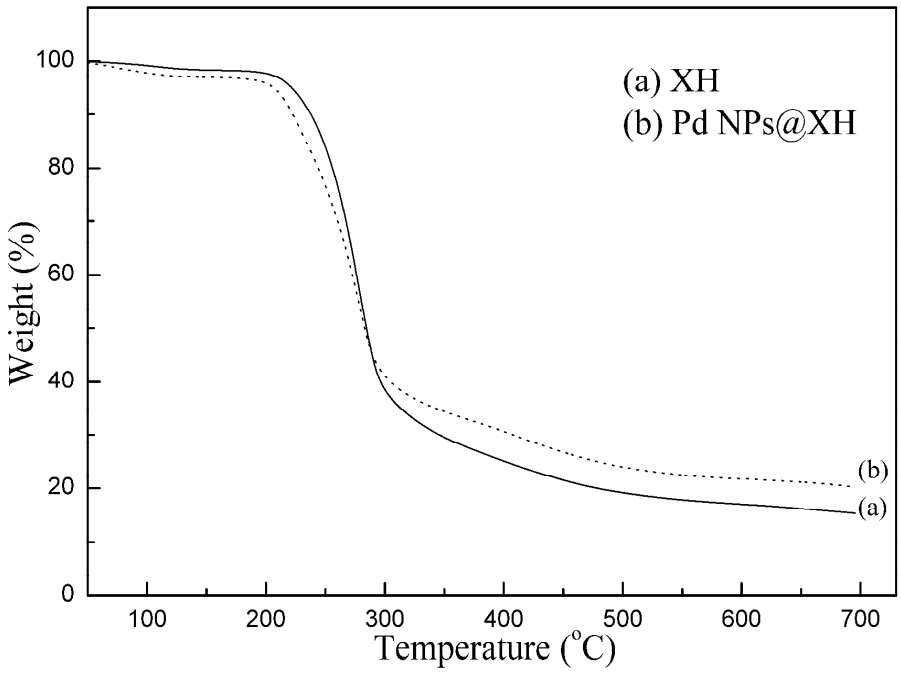

634

635 **Fig. 6** TG curves of XH and PdNPs@XH

636

637

638

639

Graphical Abstract

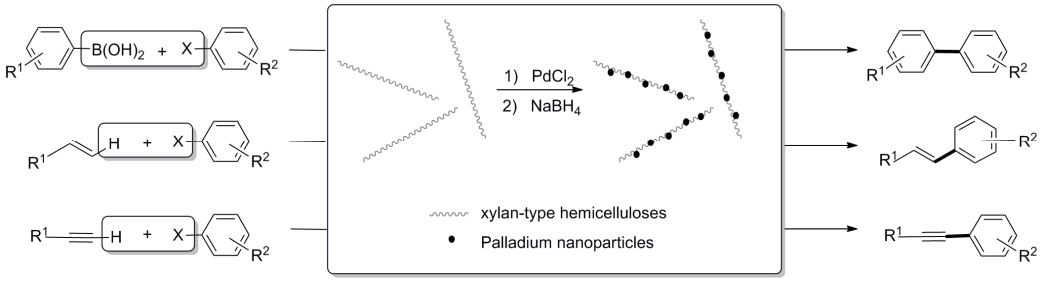

A heterogeneous catalyst was prepared by deposited palladium nanoparticle onto xylan-type hemicelluloses which is a kind of renewable biopolymer catalyst, and used as an efficient and recyclable catalyst for Suzuki, Heck, and Sonogashira cross-coupling reactions.

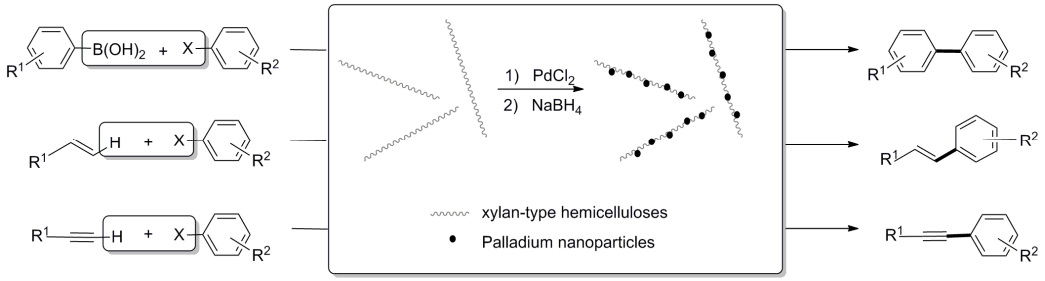

Scheme 1 Preparation of the xylan-type hemicellulose supported palladium catalyst and its applications in Suzuki, Heck, and Sonogashira reactions.

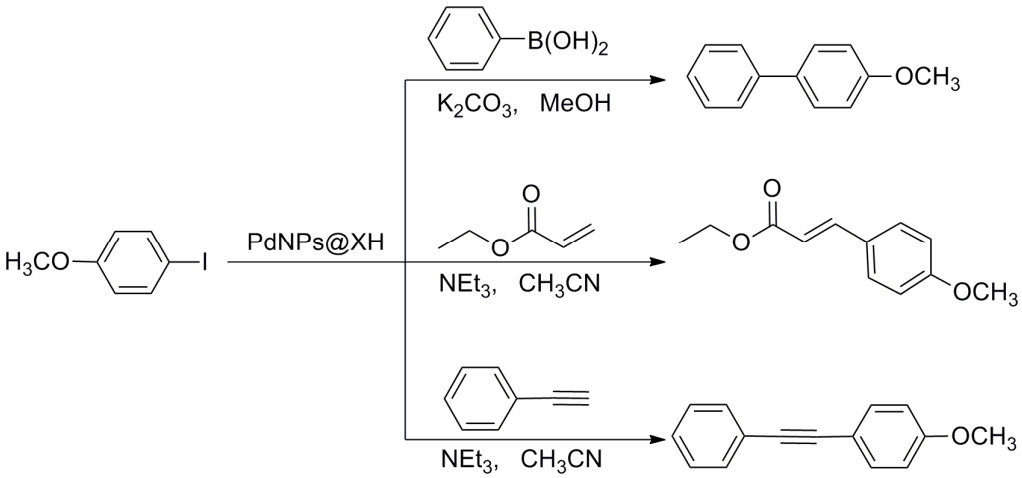

Scheme 2 PdNPs@XH catalyzed Suzuki, Heck, and Sonogashira reactions.

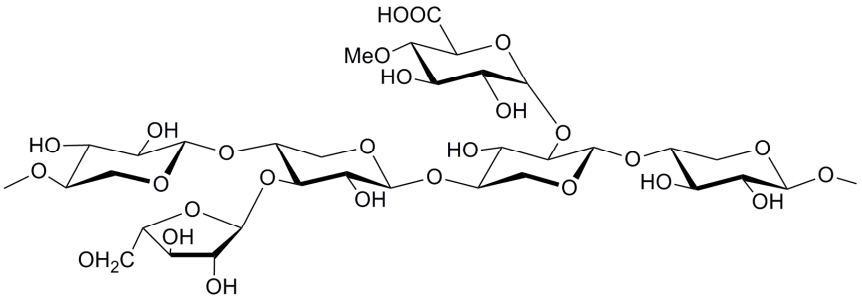

Fig. 1 Represent structure of xylan-type hemicellulose

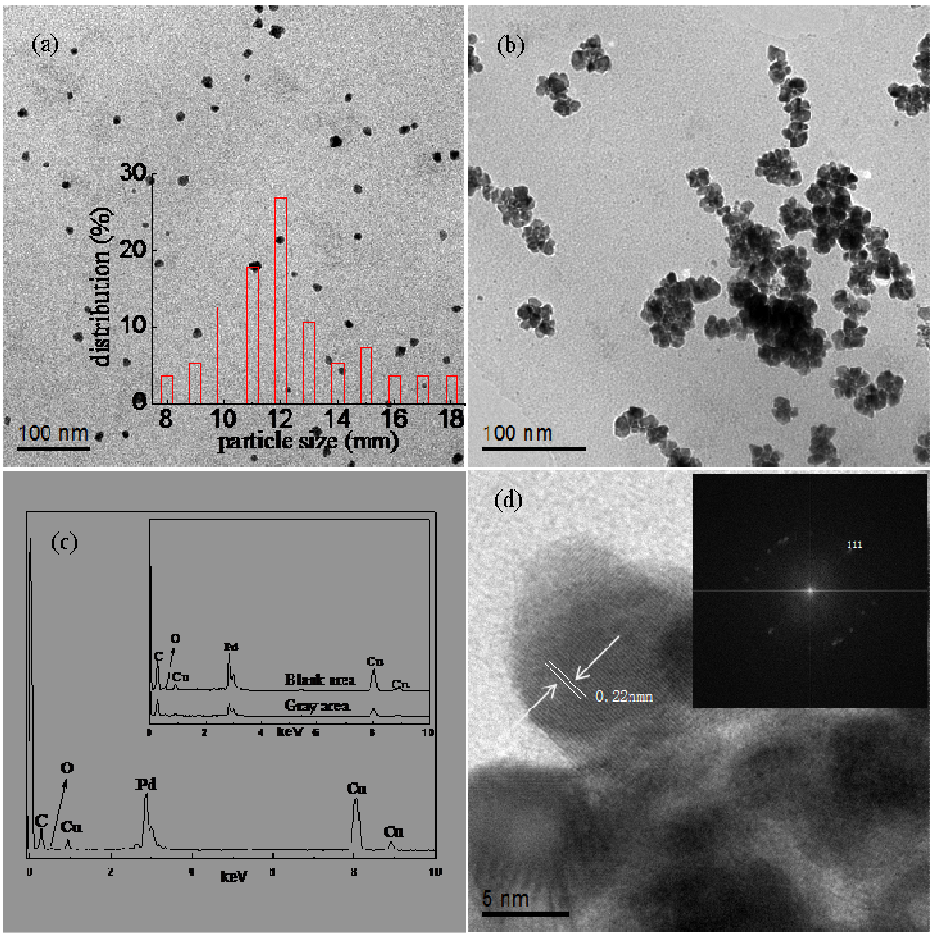

Fig. 2 TEM images: (a) Fresh PdNPs@XH and particle size distribution histogram; (b) The reused PdNPs@XH originated from Suzuki reaction for six times; (c) EDAX of PdNPs@XH and reused PdNPs@XH originated from Suzuki reaction; (d) Lattice fringe of Pd nanoparticles

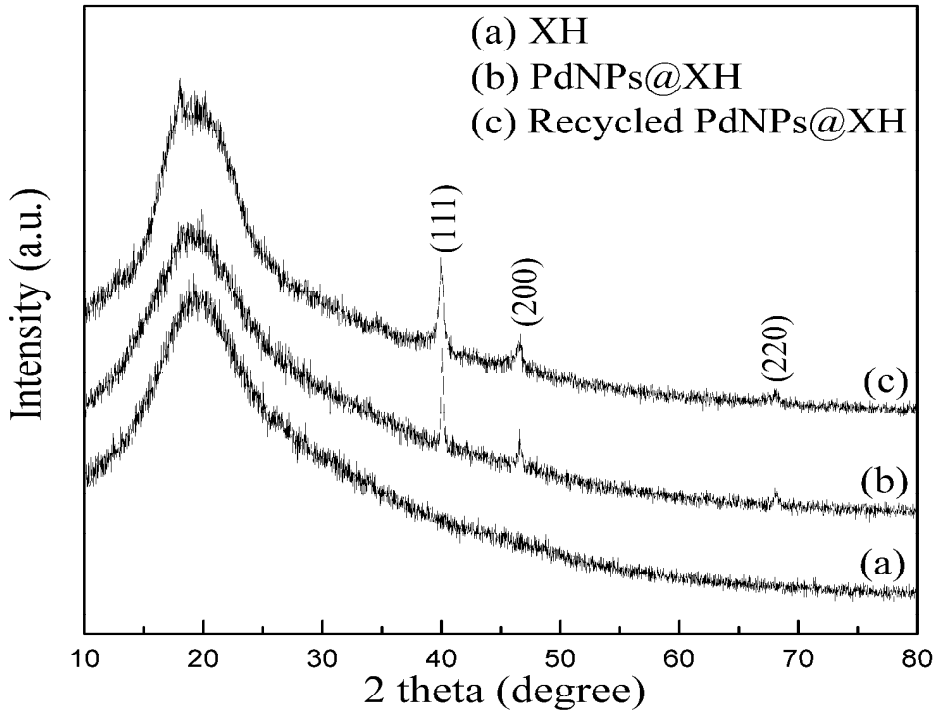

Fig. 3 XRD of XH, PdNPs@XH and recycled PdNPs@XH

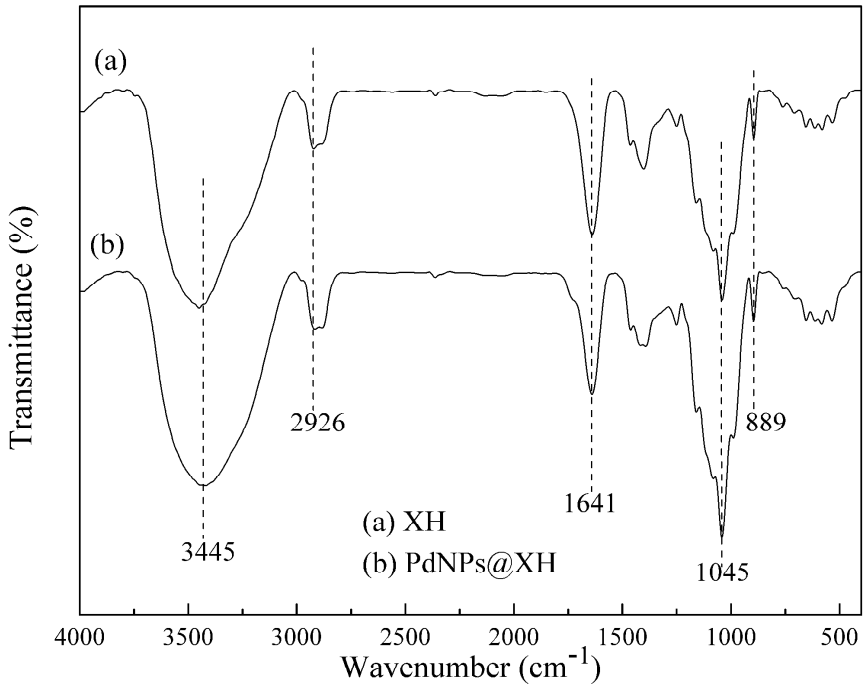

Fig. 4 FT-IR spectra of XH and PdNPs@XH

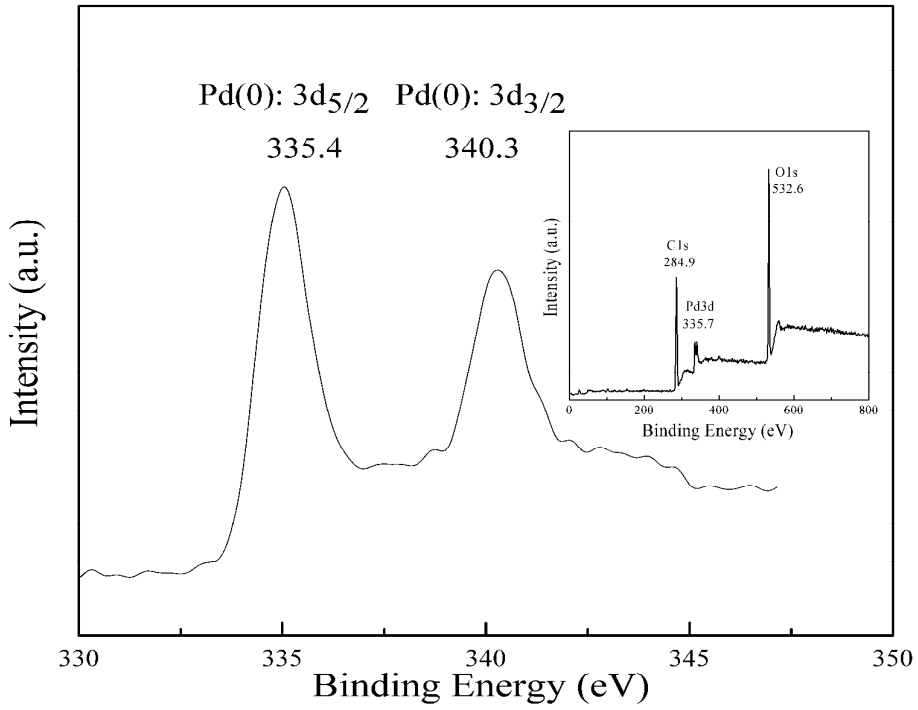

Fig. 5 XPS of PdNPs@XH

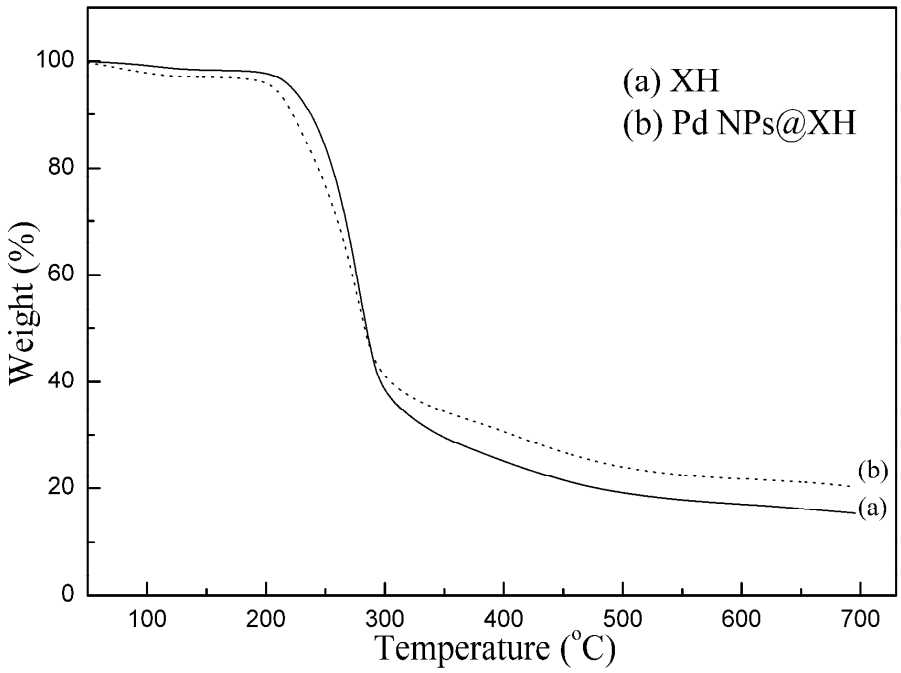

Fig. 6 TG curves of XH and PdNPs@XH